Substructure location and size effects on decentralized model updating

Xinjun Dong, Dapeng Zhu, Yang Wang *
School of Civil and Environmental Eng., Georgia Inst. of Technology, Atlanta, GA 30332, USA

ABSTRACT

To improve the simulation accuracy of the finite-element (FE) model of an as-built structure, measurement data from the actual structure can be utilized for updating the model parameters, which is termed as FE model updating. During the past few decades, most efforts on FE model updating intend to update the entire structure model altogether, while using measurement data from sensors installed throughout the structure. When applied on large and complex structural models, the typical model updating approaches may fail due to computational challenges and convergence issues. In order to reduce the computational difficulty, this paper studies a decentralized FE model updating approach that intends to update one substructure at a time. The approach divides the entire structure into a substructure (currently being instrumented and updated) and the residual structure. The Craig-Bampton transform is adopted to condense the overall structural model. The optimization objective is formulated to minimize the modal dynamic residuals from the eigenvalue equations in structural dynamics involving natural frequencies and mode shapes. This paper investigates the effects of different substructure locations and sizes on updating performance. A space frame example, which is based on an actual pedestrian bridge on Georgia Tech campus, is used to study the substructure location and size effects.

Keywords: substructure model updating, modal dynamic residuals, iterative linearization

1. INTRODUCTION

In order to simulate structural behavior under various operational loading conditions, finite element (FE) models are often constructed. Over the past few decades, significant progress has been made in FE modeling of civil structures. Nevertheless, discrepancies usually exist in structural behavior between the prediction from FE models (built according to design drawings) and actual structures in the field. For example, nominal material properties are usually adopted in FE models, while actual material properties can be different. In another example, idealized connections and support conditions are typically used in structural analysis and design, while these conditions do not exist in reality. As a result, a preliminary FE model may not accurately describe the behavior of the actual structure. To achieve higher accuracy, FE model updating can be performed based on sensor measurements from the actual structure in the field.

Numerous FE model updating methods have been developed in the past few years [3]. The discrepancies between experimental measurement and FE model are adopted as the minimization objective for FE model updating. Such discrepancy objective can be based on time histories [4], vibration modes [5], frequency response function [7], among others. Nevertheless, when applied to a high-resolution FE model of a large structure, many existing algorithms suffer computational challenges and convergence problem. The difficulties come from the fact that most of the existing algorithms operate on an entire structural model with very large amount of degrees of freedom (DOFs). In order to address the difficulties, some research activities have been devoted to substructure model updating, which focuses on updating one part of a large structure (instead of the entire structure) at a time. For instance, operating in time domain, Tee *et al*. proposed a substructure identification approach, in the context of first and second order model identification in conjunction with observer/Kalman filter and eigensystem realization [8]. In other studies, frequency spectra are adopted for substructure identification, by minimizing the difference between simulated and experimental acceleration spectra in certain frequency band [9]. Finally, towards substructure model updating, Link adopts Craig-Bampton transform, and updates the substructure model by minimizing difference between simulated and experimental modal properties [1, 6].

When applying substructure model updating, it is worth considering the appropriate selection of substructure location and size. Relevant issues include the availability of sensor instrumentation, the objective and interest of model updating, the type and size of the entire structure, the categories of updating parameters, the accuracy of the initial finite element model, *etc*. It is therefore generally difficult to provide a universal guide for selecting substructure location and size. This research conducts a preliminary study using an example space frame structure, which is based on an actual pedestrian bridge on Georgia Tech campus, to investigate the effects of substructure location and size on the substructure model updating

*yang.wang@ce.gatech.edu; phone 1 404 894-1851; http://wang.ce.gatech.edu

performance. Following the approach proposed by Zhu *et al.* [11], the residual structure is condensed through the Craig-Bampton transform. A modal dynamic residual approach is proposed as the optimization problem for model updating. An iterative linearization procedure is adopted for efficiently solving the optimization problem [2]. The rest of the paper is organized as follows. Section 2 presented the formulation of substructure modeling and model updating through the modal dynamic residual approach. Section 3 described simulation studies on a space frame structure to evaluate the performance of the proposed approach with respect to substructure location and substructure size. Section 4 provides a summary and discussion.

2. SUBSTRUCTURE MODELING AND UPDATING

This section presents the basic formulation for substructure model updating. Section 2.1 describes substructure modeling strategy following the Craig-Bampton transform. Section 2.2 describes substructure model updating through minimization of modal dynamic residual.

2.1 Substructure modeling

Figure 1 illustrates the substructure modeling strategy following Craig-Bampton transform [1]. Subscripts S, I, and R are used to denote DOFs associated with the substructure being analyzed ($\mathbf{x}_\mathrm{S}$), the interface nodes ($\mathbf{x}_\mathrm{I}$), and the residual structure ($\mathbf{x}_\mathrm{R}$), respectively. By adopting the Craig -Bampton transform [1], the dynamic behavior of the residual DOFs, $\mathbf{x}_\mathrm{R} \in \mathbb{R}^{n_\mathrm{R}}$, can be approximated by a linear combination of interface DOFs, $\mathbf{x}_\mathrm{I} \in \mathbb{R}^{n_\mathrm{I}}$, and modal coordinates of the residual structure with fixed interface, $\mathbf{q}_\mathrm{R} \in \mathbb{R}^{n_q}$. Although the size of the residual structure may be large, the number of modal coordinates, n_q, can be selected as relatively small to only reflect the first few dominant mode (i.e. $n_q << n_\mathrm{R}$).

Link [6] described a model updating method for both the substructure and the residual structure. The condensed structural model with reduced DOFs, $[\mathbf{x}_\mathrm{S} \;\; \mathbf{x}_\mathrm{I} \;\; \mathbf{q}_\mathrm{R}]^\mathrm{T}$, can be updated with selected physical and modal parameters. The condensed stiffness and mass matrix for the entire structure, $\widetilde{\mathbf{K}}$ and $\widetilde{\mathbf{M}} \in \mathbb{R}^{(n_\mathrm{S}+n_\mathrm{I}+n_q)\times(n_\mathrm{S}+n_\mathrm{I}+n_q)}$, can be written as:

$$\tilde{\mathbf{K}} = \tilde{\mathbf{K}}_0 + \sum_{j=1}^{n_\alpha} \alpha_j \mathbf{S}_{\alpha,j} + \sum_{j=1}^{n_\mathrm{I}+n_q} \zeta_j \mathbf{S}_{\zeta,j} \tag{1}$$

$$\tilde{\mathbf{M}} = \tilde{\mathbf{M}}_0 + \sum_{j=1}^{n_\beta} \beta_j \mathbf{S}_{\beta,j} + \sum_{j=1}^{n_\mathrm{I}+n_q} \eta_j \mathbf{S}_{\eta,j} \tag{2}$$

by defining

$$\tilde{\mathbf{K}}_0 = \begin{bmatrix} \begin{bmatrix} \mathbf{K}_{\mathrm{S}0} \end{bmatrix} & \mathbf{0} \\ & \mathbf{0} \\ \mathbf{0} \quad \mathbf{0} & \mathbf{0} \end{bmatrix} + \begin{bmatrix} \mathbf{0} & \mathbf{0} \quad \mathbf{0} \\ \mathbf{0} & \\ \mathbf{0} & \begin{bmatrix} \tilde{\mathbf{K}}_{\mathrm{R}0} \end{bmatrix} \end{bmatrix} \begin{array}{c} \mathbf{x}_\mathrm{S} \\ \mathbf{x}_\mathrm{I} \\ \mathbf{q}_\mathrm{R} \end{array} \tag{3}$$

$$\tilde{\mathbf{M}}_0 = \begin{bmatrix} \begin{bmatrix} \mathbf{M}_{\mathrm{S}0} \end{bmatrix} & \mathbf{0} \\ & \mathbf{0} \\ \mathbf{0} \quad \mathbf{0} & \mathbf{0} \end{bmatrix} + \begin{bmatrix} \mathbf{0} & \mathbf{0} \quad \mathbf{0} \\ \mathbf{0} & \\ \mathbf{0} & \begin{bmatrix} \tilde{\mathbf{M}}_{\mathrm{R}0} \end{bmatrix} \end{bmatrix} \begin{array}{c} \mathbf{x}_\mathrm{S} \\ \mathbf{x}_\mathrm{I} \\ \mathbf{q}_\mathrm{R} \end{array} \tag{4}$$

where $\mathbf{K}_{\mathrm{S}0}$ and $\mathbf{M}_{\mathrm{S}0}$ are the stiffness and mass matrices of the substructure and used as initial starting points in the model updating; $\widetilde{\mathbf{K}}_{\mathrm{R}0}$ and $\widetilde{\mathbf{M}}_{\mathrm{R}0}$ are the initial stiffness and mass matrices of the condensed residual structure model; α_j and β_j correspond to the physical system parameters inside the substructure to be updated, such as elastic modulus and density of substructure elements; n_α and n_β represent the total number of the corresponding physical parameters to be updated; ζ_j and η_j are the modal parameters of the residual structure to be updated. $\mathbf{S}_{\alpha,j}$, $\mathbf{S}_{\beta,j}$, $\mathbf{S}_{\zeta,j}$ and $\mathbf{S}_{\eta,j}$ represent the constant sensitivity matrices corresponding to variables α_j, β_j, ζ_j and η_j, respectively. For brevity, these variables will be referred to in vector form as $\boldsymbol{\alpha} \in \mathbb{R}^{n_\alpha}$, $\boldsymbol{\beta} \in \mathbb{R}^{n_\beta}$, $\boldsymbol{\zeta} \in \mathbb{R}^{n_\mathrm{I}+n_q}$ and $\boldsymbol{\eta} \in \mathbb{R}^{n_\mathrm{I}+n_q}$. Detailed formulations can be found in [11].

2.2 Substructure model updating through minimization of modal dynamic residual

To update the substructure model, a modal dynamic residual approach is presented in this study. The model updating approach aims to minimize the summation of modal dynamic residual of the generalized eigenvalue equation.

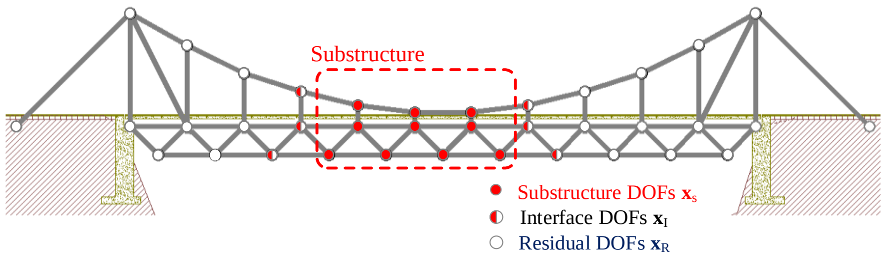

Figure 1. Illustration of substructure modeling strategy

$$\underset{\boldsymbol{\alpha},\boldsymbol{\beta},\boldsymbol{\zeta},\boldsymbol{\eta},\boldsymbol{\psi}_{\text{unmeas}}}{\text{minimize}} \quad \sum_{j=1}^{n_{\text{meas}}} \left\| \left(\tilde{\mathbf{K}}(\boldsymbol{\alpha},\boldsymbol{\zeta}) - \omega_j^2 \tilde{\mathbf{M}}(\boldsymbol{\beta},\boldsymbol{\eta}) \right) \begin{Bmatrix} \boldsymbol{\psi}_{\text{meas},j} \\ \boldsymbol{\psi}_{\text{unmeas},j} \end{Bmatrix} \right\|^2 \tag{5}$$

where $\|\cdot\|$ denotes any norm function; n_{meas} denotes the number of measured modes from experiments; ω_j denotes the j-th modal frequency extracted from experimental data; $\boldsymbol{\psi}_{\text{meas},j}$ denotes the entries in the j-th mode shape that correspond to measured (instrumented) DOFs; $\boldsymbol{\psi}_{\text{unmeas},j}$ corresponds to unmeasured DOFs; $\boldsymbol{\alpha}$, $\boldsymbol{\beta}$, $\boldsymbol{\zeta}$ and $\boldsymbol{\eta}$ are the selected parameters to be updated (see Eq. (1) and (2)).

In summary, the optimization variables are system parameters $\boldsymbol{\alpha}$, $\boldsymbol{\beta}$, $\boldsymbol{\zeta}$, $\boldsymbol{\eta}$ and the mode shape entries corresponding to unmeasured DOFs, $\boldsymbol{\psi}_{\text{unmeas},j}$ ($j = 1,\ldots, n_{\text{meas}}$). Eq. (5) leads to a complex nonlinear optimization problem that is generally difficult to solve. An iterative linearization procedure for efficiently solving the optimization problem is adopted in this study, similar to [2]. Figure 2 shows the pseudo code of the procedure. Each iteration step involves two operations, modal expansion and parameter updating. The operation (i) is modal expansion for unmeasured DOFs, where system parameters ($\boldsymbol{\alpha}$, $\boldsymbol{\beta}$, $\boldsymbol{\zeta}$ and $\boldsymbol{\eta}$) are treated as constant. When model parameters are held constant, $\boldsymbol{\psi}_{\text{unmeas},j}$ ($j = 1,\ldots, n_{\text{meas}}$) become the optimization variables in Eq. (5). The operation (ii) at each iteration step is the updating of system parameters ($\boldsymbol{\alpha}$, $\boldsymbol{\beta}$, $\boldsymbol{\zeta}$ and $\boldsymbol{\eta}$) using the expanded mode shapes. Thus, $\boldsymbol{\psi}_{\text{unmeas},j}$ ($j = 1,\ldots, n_{\text{meas}}$) is held as constant in operation (ii), and the system parameters are optimization variables. When 2-norm is used in Eq. (5), the optimization problem in both operations becomes a simple least square problem.

3. NUMERICAL EXAMPLES

Figure 3 shows the numerical model of a space frame bridge, which is based on an actual pedestrian bridge on Georgia Tech campus. The space frame model contains 46 nodes, each node with six DOFs. Although mainly a frame structure, the segment cross bracings in top plane and two side planes are truss members. Transverse and vertical springs (k_y and k_z) are allocated at both ends of the frame structure to simulate non-ideal boundary conditions. In this study, it is assumed to have accurate information on structural mass, so mass parameters $\boldsymbol{\beta}$ is not among the updating parameters for each substructure model updating. Table 1 summarizes the structural stiffness parameters of the model. The parameters are divided into three categories. The first category contains six parameters (starting from top in the table), which are elastic moduli of the diagonal bracing truss members in top plane and the frame members along the entire length of the frame structure. The second category contains ten parameters, which are the elastic moduli of diagonal bracing truss members in

```
start with α, β, ζ and η = 0 (meaning M and K start with initial values at M0 and K0) ;
REPEAT {
    (i) hold α, β, ζ and η as constant and minimize Eq.(5) over variable ψunmeas,j (j = 1,…,nmeas) ;
   (ii) hold ψunmeas,j (j = 1,…,nmeas) as constant and minimize Eq.(5) over variables α, β, ζ and η ;
} UNTIL convergence ;
```

Figure 2. Pseudo code of the iterative linearization procedure

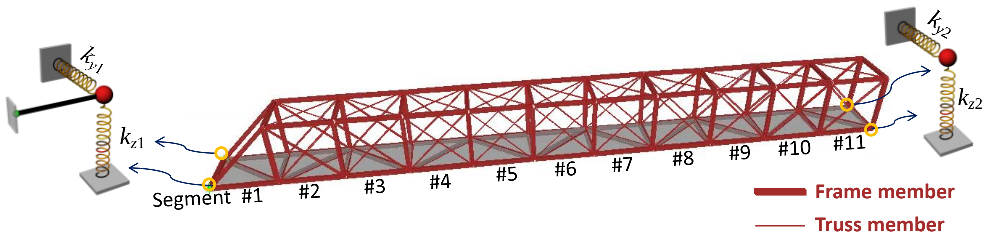

Figure 3. Illustration of substructure modeling strategy

Table 1 Structure stiffness parameters

Updating parameter			Initial value	Actual value	Change (%)
Elastic moduli of members along the frame structure (kips/in^2)	Frame members	E_1 – Longitudinal top chord	29,000	30,450	5
		E_2 – Longitudinal bottom chord	29,000	30,450	5
		E_3 – Vertical members	29,000	27,550	-5
		E_4 – Transverse top chord	29,000	26,100	-10
		E_5 – Transverse & diagonal bottom chord	29,000	30,450	5
	Truss members	E_6 – Diagonal bracings in top plane	29,000	27,550	-5
Elastic moduli of side-plane diagonal bracings (truss members) for each segment (kips/in^2)	E_{S2} – 2nd segment		29,000	26,100	-10
	E_{S3} – 3rd segment		29,000	26,100	-10
	E_{S4} – 4th segment		29,000	26,100	-10
	E_{S5} – 5th segment		29,000	27,550	-5
	E_{S6} – 6th segment		29,000	27,550	-5
	E_{S7} – 7th segment		29,000	27,550	-5
	E_{S8} – 8th segment		29,000	24,650	-15
	E_{S9} – 9th segment		29,000	26,100	-10
	E_{S10} – 10th segment		29,000	27,550	-5
	E_{S11} – 11th segment		29,000	27,550	-5
Support springs (kips/in)	k_{y1} – Left transverse		200	140	-30
	k_{z1} – Left vertical		500	800	60
	k_{y2} – Right transverse		200	140	-30
	k_{z2} – Right vertical		500	800	60

two side planes for different segments. The third category contains stiffness parameters of the four types of support springs. Table 1 provides initial (nominal) values for all parameters, as starting point for model updating. The table also lists actual values, which ideally are to be identified. The relative changes from initial to actual values, to be identified, are also listed. Although the assignment of actual values in Table 1 is intended to be somewhat arbitrary, as often happening in practice, it is assumed that the initial model has higher accuracy for material properties (with maximum relative difference of -15% for E_{S8}), and lower accuracy for the stiffness of support springs (with maximum relative difference of 60% for k_{z1} and k_{z2}).

The proposed substructure model updating approach has been validated on the same structure in a previous study [10]. This research aims to evaluate the performance of the proposed approach with respect to substructure location, and to substructure size. Section 3.1 and Section 3.2 compare the model updating results of different substructure sizes and substructure locations, respectively.

3.1 Investigation on substructure location

The entire space frame model is divided into four substructures with similar size, as shown in Figure 4. Substructure #1 contains segments 1~3, substructure #2 contains segments 4~6, substructure #3 contains segments 7~9, and substructure #4 contains segments 10~11. Substructure model updating is conducted on each substructure separately, when the residual structure contains the rest of the structure. For example, when updating substructure #2, the residual structure contains

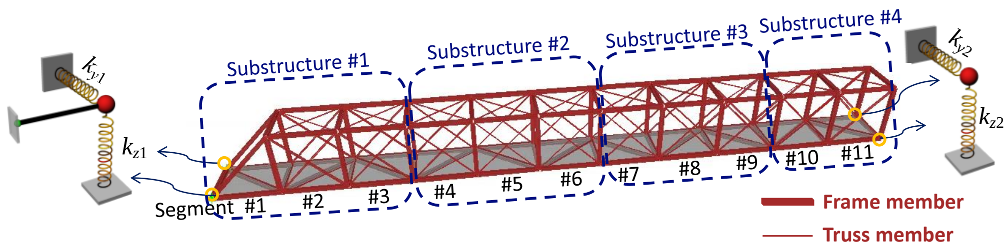

Figure 4. Substructures at various locations

substructures #1, #3 and #4. For practicality, it is also assumed only translational DOFs of the substructure and interface nodes are instrumented with sensors for capturing substructure vibration modes; rotational DOFs are not measured. In addition, regardless of the substructure selection, no measurement is required on the residual structure. Modal frequencies and substructure mode shapes of the simulated actual structure (ω_j and $\boldsymbol{\psi}_{\text{meas},j}$) are used as "experimental data".

For model condensation, dynamic response of the residual structure for each substructure model updating is approximated using twenty modal coordinates, i.e. n_q = 20. All substructure models contain updating parameters along the entire structure, such as the five elastic moduli of the frame members (E_1~E_5), and the elastic moduli of top bracing truss members (E_6). Meanwhile, each substructure model also contains its own location-dependent updating parameters. For example, substructure #1 contains elastic moduli of side-bracing truss members at the 2nd and 3rd segments (E_{S2} and E_{S3}), and the spring stiffness values at the left support (k_{y1} and k_{z1}). Substructure #2 contains elastic moduli of side-bracing truss members at the 4th, 5th, and 6th segments (E_{S4}, E_{S5} and E_{S6}). Substructure #3 contains elastic moduli of side-bracing truss members at the 7th, 8th, and 9th segments (E_{S7}, E_{S8} and E_{S9}). Finally, substructure #4 contains elastic moduli of side-bracing truss members at the 10th and 11th segments (E_{S10} and E_{S11}), and the spring stiffness values at the right support (k_{y1} and k_{z1}).

Table 2 summarizes the updating results for all substructure models, assuming five measured modes are available for updating of each substructure. For each substructure updating, most of the updated parameter changes are close to the ideal percentages listed in Table 1. The parameters of the corresponding residual structure cannot be updated, and are marked with "—". Note that E_4 is not used to compare the performance, because it is proved to be less sensitive to translational DOFs [10]. Therefore, E_4 will not be included when evaluating the model updating performance hereinafter.

To quantify the updating accuracy for each substructure updating, Figure 5 plots the relative updating errors of the physical parameters in each substructure, i.e. relative difference of updated values from the actual parameter values (without E_4). The updating errors are generally small for each substructure updating (most errors are within -1% ~ +1%). An exception is E_3 in substructure #2, with a larger error of +2.83%. To further quantify the performance, the average values of the relative updating errors for each substructure are calculated and shown in the title of each plot in Figure 5, where substructure #2 gives the lowest updating accuracy (with an average error of 0.9%).

Table 2 Updated stiffness parameter changes (%) for the substructure models with five available modes

Substructure	**Frame member**					**Spring**			
	E_1	E_2	E_3	E_4	E_5	k_{y1}	k_{z1}	k_{y1}	k_{z2}
#1	4.21	4.17	-5.61	-5.76	4.16	-30.54	59.01	—	—
#2	4.85	4.24	-2.17	-3.76	4.06	—	—	—	—
#3	5.47	4.53	-4.85	-7.19	4.75	—	—	—	—
#4	4.44	4.29	-5.23	-5.43	4.08	—	—	-30.48	-59.42

Substructure	**Truss member**										
	E_6	E_{S2}	E_{S3}	E_{S4}	E_{S5}	E_{S6}	E_{S7}	E_{S8}	E_{S9}	E_{S10}	E_{S11}
#1	-6.24	-10.68	-10.94	—	—	—	—	—	—	—	—
#2	-4.14	—	—	10.52	-5.41	-5.73	—	—	—	—	—
#3	-4.54	—	—	—	—	—	-5.43	-14.82	-10.15	—	—
#4	-5.21	—	—	—	—	—	—	—	—	-5.58	-5.46

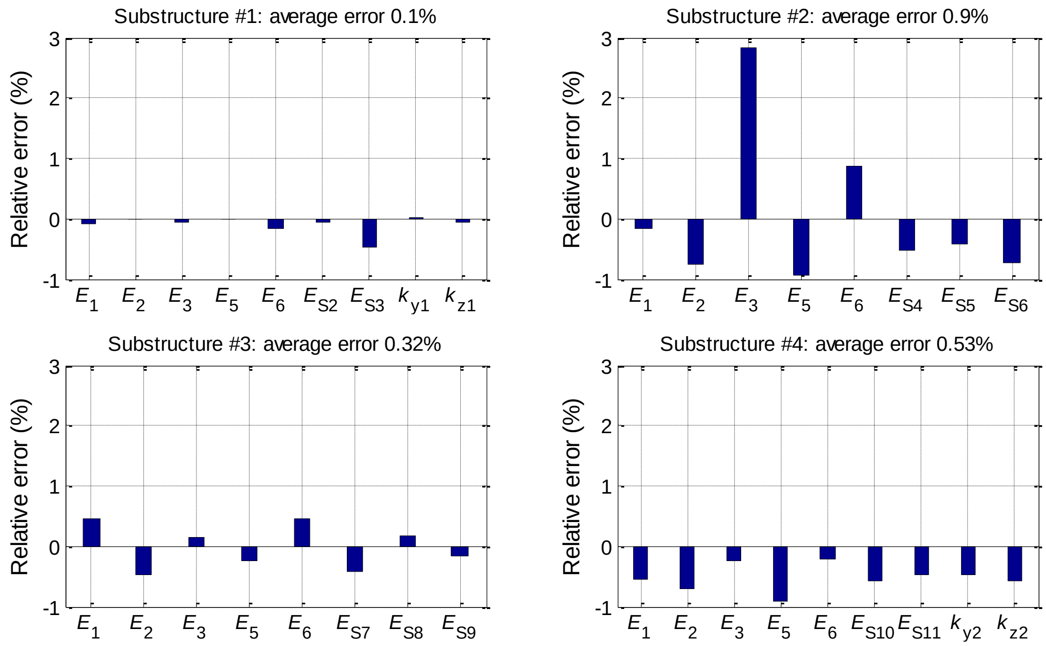

Figure 5. Relative errors of the updated parameters for substructures at various locations

Reviewing the substructure locations in Figure 5, it is easy to see that the substructures #1 and #4 are located close to the two ends of the frame structure, and contains the parameters with most inaccurate initial values (stiffness of the support springs). Substructure #3 contains the cross bracing truss members with the most inaccurate initial value (E_{S8}), where initial value is off from actual value by -15%. These inaccurate parameters get directly updated in the updating procedure of these three substructures. Meanwhile, substructure #2 is located close to the middle of the frame structure. The parameters with most inaccurate initial values are in the corresponding residual structure of substructure #2, and thus, cannot be directly updated. The residual structure is updated using modal parameters, based on the assumption that parameter changes in the actual residual structure from initial values do not significantly alter the modal properties of the residual structure. Therefore, those parameters with most inaccurate initial values in the residual structure cause more difficulties when updating substructures #2. In summary, the simulation illustrates that to obtain higher updating accuracy, a substructure can be located to contain parameters associated with least prior knowledge (which tend to have largest initial errors), so that these parameters can be updated together with the substructure.

3.2 Investigation on substructure size

Choosing an appropriate substructure size is another interesting issue for substructure updating. A smaller substructure contains less number of DOFs, and thus the updating requires less computation efforts. However, decrease of substructure size increases the discrepancy between of the simulated residual structure and the actual residual structure. This subsection conducts a preliminary study on the space frame structure to verify updating accuracy with different sizes of the substructure.

The substructure containing the first three segments has been studied in [10] (Figure 6). This study extends to two additional examples with different substructure sizes. The first one adopts a smaller substructure with the first two segments (Figure 7), containing 6 substructure nodes and 4 interface nodes. The second one adopts a larger substructure with the first four segments (Figure 8), containing 14 substructure nodes and 4 interface nodes. For model condensation, dynamic response of the residual structure for each substructure model is approximated using twenty modal coordinates, i.e. n_q = 20. Similar as Section 3.1, it is assumed only translational DOFs of the substructure and interface nodes are instrumented with sensors for capturing substructure vibration modes; rotational DOFs are not measured.

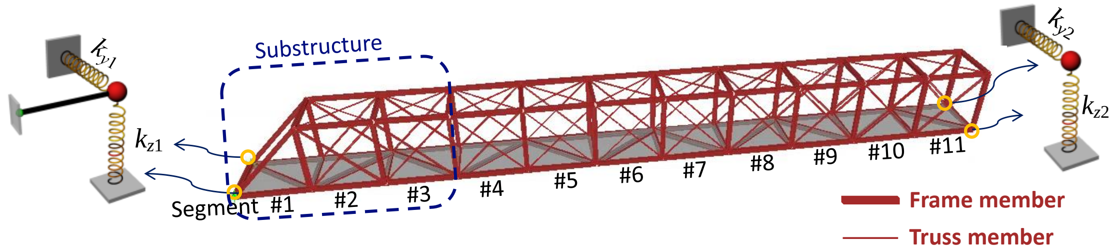

Figure 6. Three-segment substructure

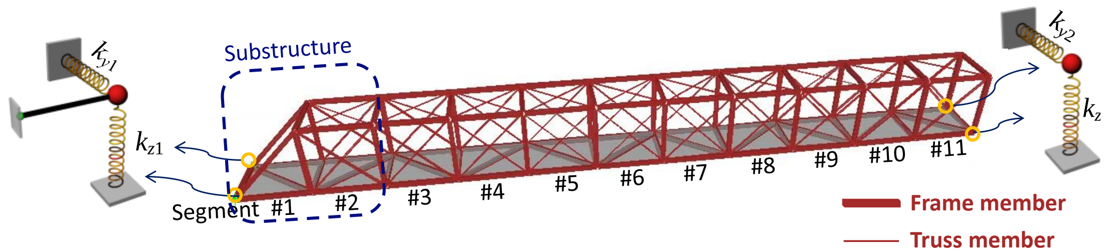

Figure 7. Two-segment substructure

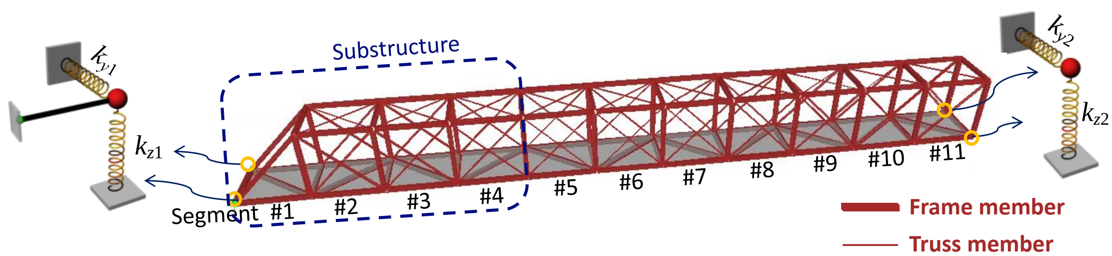

Figure 8. Four-segment substructure

The stiffness parameters for all three examples are similar to each other. They all contain the five elastic moduli of the frame members (E_1~E_5), the elastic moduli of top bracing truss members (E_6), and the spring stiffness values at the left support (k_{y1} and k_{z1}). The difference is that the two-segment substructure only includes the elastic moduli of side-bracing truss members at the 2nd segments (E_{S2}); the three-segment substructure includes the elastic moduli of side-bracing truss members at the 2nd segments (E_{S2}) and the 3rd segments (E_{S3}); the four-segment substructure includes the elastic moduli of side-bracing truss member at the 2nd, 3rd, and 4th segments (E_{S2}, E_{S3}, E_{S4}).

Table 3 summarizes the updating results for the three-segment substructure model, including scenarios when 3, 4, 5 or 6 measured modes are available for model updating. The results are presented in terms of relative change percentages from initial values. For every available number of modes, most of the updated parameter changes are close to the ideal percentages listed in Table 1. Similar to Section 3.1 the non-sensitive updating parameter E_4 is not considered for evaluating the updating performance. For clear demonstration of updating accuracy, Figure 9 plots the relative errors of the updating results, i.e. relative difference of updated values from the actual parameter values, for different number of available modes (without E_4). The figure shows that the updating results accurately identify all other substructure stiffness parameters. In addition, the updating accuracy generally improves when more measured modes are available.

Table 4 summarizes the updating results for the two-segment substructure model. The results are presented in terms of relative change percentages from initial values. When three modes are available, most of the updated parameter changes are quite different to the actual percentages listed in Table 1. With more available modes, the updating accuracy improves.

Table 3 Updated parameter changes (%) for substructure elements on the three-segment substructure model

Available modes	**Frame member**					**Truss member**			**Spring**	
	E_1	E_2	E_3	E_4	E_5	E_6	E_{S2}	E_{S3}	k_{y1}	k_{z1}
3 modes	3.41	2.94	-6.35	-5.51	2.90	-6.60	-11.48	-12.00	-31.42	57.63
4 modes	4.81	4.23	-5.03	-4.38	4.21	-5.23	-10.33	-10.76	-30.55	59.83
5 modes	4.93	4.36	-5.02	-4.40	4.33	-5.82	-10.20	-10.98	-30.47	59.92
6 modes	4.96	4.38	-4.97	-4.03	4.36	-6.34	-10.19	-12.39	-30.42	59.98

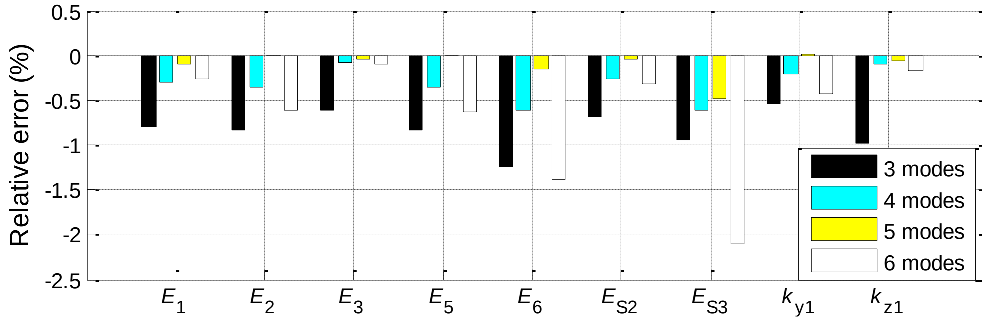

Figure 9. Relative errors of the updated parameters for the three-segment substructure

Figure 10 plots the relative errors of the updating results (excluding E_4) for different numbers of available modes. The figure also shows the updating accuracy significantly improves when more measured modes are available.

Table 5 summarizes the updating results for the four-segment substructure model. For every available number of modes, most of the updated parameter changes are close to the ideal percentages listed in Table 1. Figure 11 plots the relative errors of the updating results (excluding E_4) for different numbers of available modes. The maximum error is only 0.46% for E_6 with six available modes, which indicates that reasonable results can be achieved for all available modes. The figure also shows the updating accuracy is generally improved when more measured modes are available.

Table 4 Updated parameter changes (%) for substructure elements on the two-segment substructure model

Available modes	**Frame member**					**Truss member**		**Spring**	
	E_1	E_2	E_3	E_4	E_5	E_6	E_{S2}	k_{y1}	k_{z1}
3 modes	-1.12	-2.69	-10.26	-10.29	-2.85	-11.88	-15.85	-35.19	51.09
4 modes	2.99	2.70	-6.65	-7.03	2.66	-7.96	-11.96	-31.53	57.23
5 modes	4.76	4.77	-5.15	-5.67	4.75	-5.59	-10.28	-30.14	59.76
6 modes	4.65	4.36	-5.05	-5.20	4.35	-5.91	-10.62	-30.44	59.91

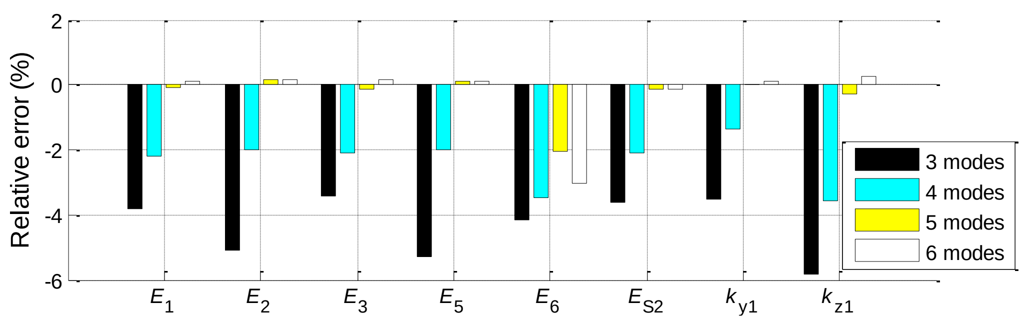

Figure 10. Relative errors of the updated parameters for the two-segment substructure

Table 5 Updated parameter changes (%) for substructure elements on the four-segment substructure model

Available modes	**Frame member**					**Truss member**				**Spring**	
	E_1	E_2	E_3	E_4	E_5	E_6	E_{S2}	E_{S3}	E_{S4}	k_{y1}	k_{z1}
3 modes	4.87	4.80	-4.96	-5.19	4.79	-5.14	-10.13	-10.12	-10.03	-30.12	60.10
4 modes	4.89	4.83	-4.89	-5.23	4.82	-5.19	-10.12	-10.07	-10.01	-30.09	60.22
5 modes	4.88	4.86	-5.07	-6.01	4.85	-4.64	-10.07	-10.02	-10.10	-30.08	59.89
6 modes	5.06	4.76	-4.92	-5.68	4.74	-4.53	-10.01	-9.94	-10.25	-30.18	60.14

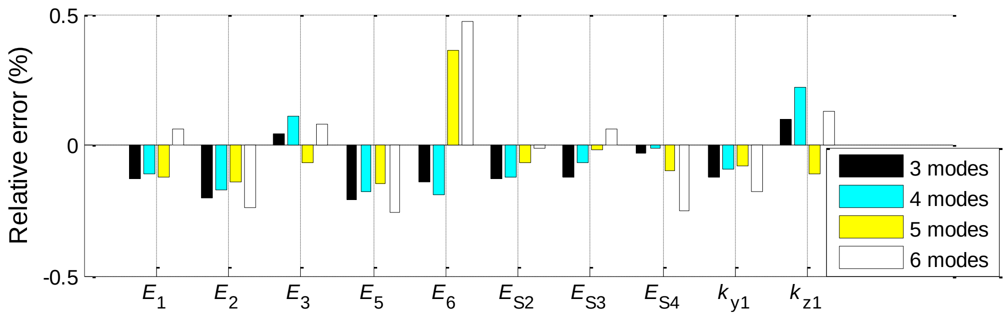

Figure 11. Relative errors of the updated parameters for the four-segment substructure

Comparing Figure 9, Figure 10, and Figure 11, it can be concluded that the updating accuracy generally increases with a larger substructure size, especially for a small number of available modes. The comparison also indicates that when more measured modes are available, the updating accuracy are satisfactory for all three different substructure sizes.

4. SUMMARY & CONCLUSION

This paper studies substructure model updating through minimization of modal dynamic residual. Craig-Bampton transform is adopted to condense the entire structural model into the substructure (currently being instrumented and to be updated) and the residual structure. Finite element model of the substructure remains at high resolution, while dynamic behavior of the residual structure is approximated using only a limited number of dominant mode shapes. To update the condensed structural model, physical parameters in the substructure and modal parameters of the residual structure are chosen as optimization variables; minimization of the modal dynamic residual is chosen as the optimization objective. An iterative linearization procedure is adopted for efficiently solving the optimization problem.

The performance of the proposed substructure model updating approach is investigated through numerical simulation of the space frame structure with respect to substructure location and to substructure size. With respect to location, four substructures of similar size are selected at different locations. The simulations show that three substructures covering parameters with least prior knowledge give more accurate updating results, because in this way, these parameters are directly updated together with the substructures. With respect to substructure size, three different sizes of substructure are simulated. With sensors of similar spatial density instrumented on all substructure and interface nodes, the results indicate that the updating accuracy generally increases with larger substructure size, especially when a smaller number of measured modes are available. When the substructure size is too small, the updating accuracy can be unacceptable when very small number of modes are available. When more measured modes are available, the updating accuracy are satisfactory for all three substructure sizes.

5. ACKNOWLEDGEMENTS

This research is partially sponsored by the National Science Foundation (#CMMI-1150700 and #CMMI-1041607), the Research and Innovative Technology Administration of US DOT (#DTRT12GUTC12), and Georgia DOT (#RP12-21). Any opinions, findings, and conclusions or recommendations expressed in this publication are those of the authors and do not necessarily reflect the view of the sponsors.

REFERENCES

[1] Craig, R. R., Jr. and Bampton, M. C. C., "Coupling of substructures of dynamics analyses," AIAA Journal, 6(7), 1313-1319 (1968).

[2] Farhat, C. and Hemez, F. M., "Updating finite element dynamic models using an element-by-element sensitivity methodology," AIAA Journal, 31(9), 1702-1711 (1993).

[3] Friswell, M. I. and Mottershead, J. E., [Finite element model updating in structural dynamics], Kluwer Academic Publishers, Dordrecht; Boston (1995).

[4] Hoshiya, M. and Saito, E., "Structural identification by extended kalman filter," Journal of Engineering Mechanics, 110(12), 1757-1770 (1984).

[5] Jaishi, B. and Ren, W. X., "Damage detection by finite element model updating using modal flexibility residual," Journal of Sound and Vibration, 290(1-2), 369-387 (2006).

[6] Link, M., "Updating analytical models by using local and global parameters and relaxed optimisation requirements," Mechanical Systems and Signal Processing, 12(1), 7-22 (1998).

[7] Sipple, J. D. and Sanayei, M., "Finite element model updating using frequency response functions and numerical sensitivities," Structural Control and Health Monitoring, 21(5), 784-802 (2014).

[8] Tee, K. F., Koh, C. G. and Quek, S. T., "Substructural first- and second-order model identification for structural damage assessment," Earthquake Engineering & Structural Dynamics, 34(15), 1755-1775 (2005).

[9] Zhang, D. and Johnson, E. A., "Substructure identification for shear structures II: Controlled substructure identification," Structural Control and Health Monitoring, 20(5), 821-834 (2013).

[10] Zhu, D., Dong, X. and Wang, Y., "Substructure finite element model updating of a space frame structure by minimization of modal dynamic residual," Proceedings of the Sixth World Conference on Structural Control and Monitoring (6WCSCM), (2014).

[11] Zhu, D., Dong, X. and Wang, Y., "Substructure model updating through iterative minimization of modal dynamic residual," Proceedings of SPIE, Nondestructive Characterization for Composite Materials, Aerospace Engineering, Civil Infrastructure, and Homeland Security, (2014).